

SUPPLEMENTARY INFORMATION

for

Mechanistic Insights into the Co-Recovery of Nickel and Iron via Integrated Carbon Mineralization of Serpentinized Peridotite by Harnessing Organic Ligands

*Shreya Katre,^{ab} Prince Ochonma,^c Hassnain Asgar,^a Archana M Nair,^b Ravi K^b
and Greeshma Gadikota^{*ac}*

*^aSchool of Civil and Environmental Engineering, Cornell University, Ithaca, NY
14853 USA*

*^bDepartment of Civil Engineering, Indian Institute of Technology, Guwahati,
Assam 781039 India*

*^cSmith School of Chemical and Biomolecular Engineering, Cornell University,
Ithaca, NY 14853 USA*

* Corresponding Author. Phone: +1 607-255-4796. E-mail: gg464@cornell.edu

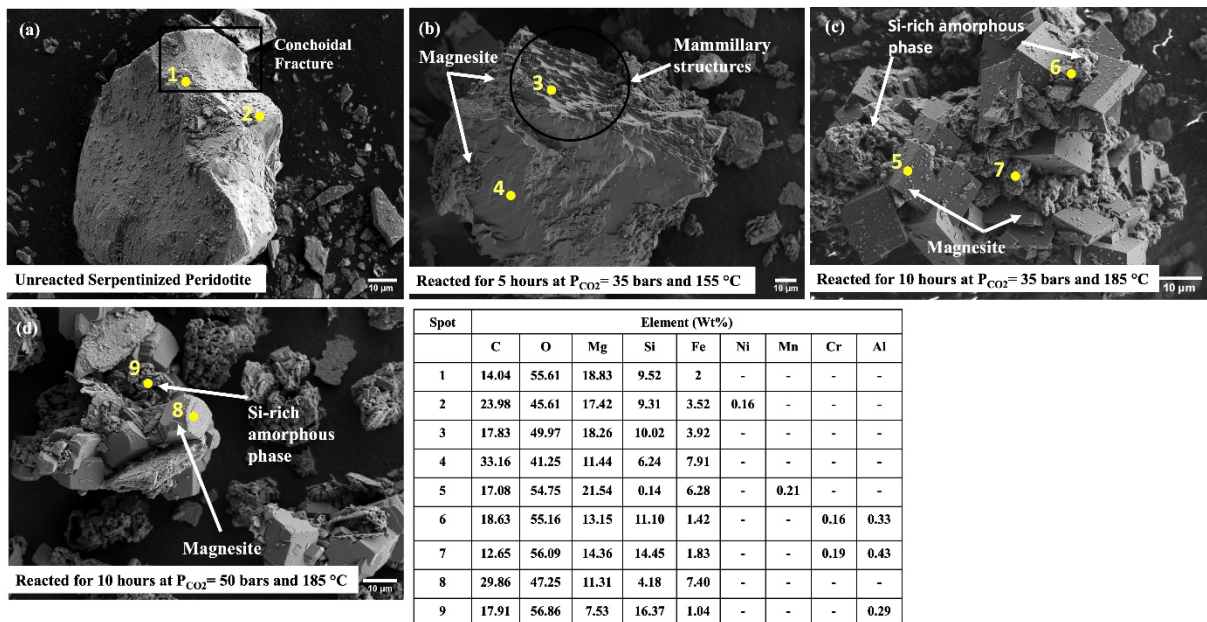


Figure S1. SEM-EDS analysis of carbonate-bearing solids for a) unreacted serpentinized peridotite (Spots 1 and 2) and carbonated solids b) reacted for 5 hours at $P_{\text{CO}_2} = 35$ bars and 155°C (Spots 3 and 4) c) reacted for 10 hours at $P_{\text{CO}_2} = 35$ bars and 185°C (Spots 5,6 and 7) d) reacted for 10 hours at $P_{\text{CO}_2} = 50$ bars and 185°C (Spots 8 and 9) using 0.1 M Na_2EDTA chelating agent + 2 M NaHCO_3 , slurry density of 15 wt% and a stirring speed of 500 rpm

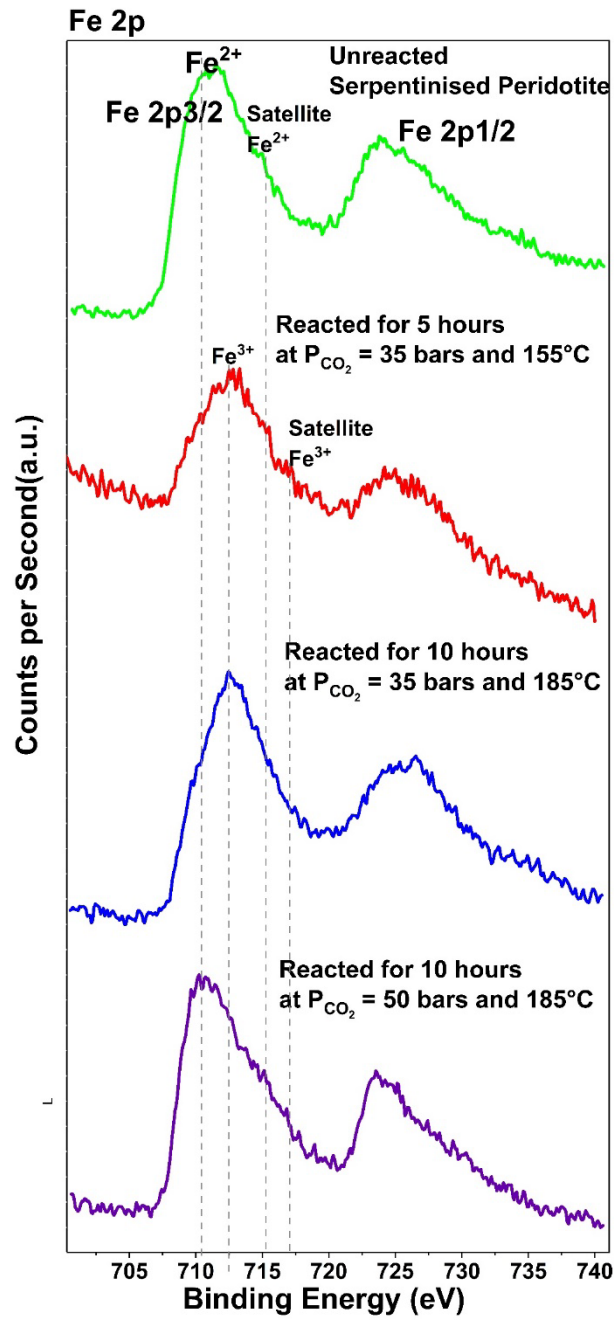


Figure S2. XPS Fe 2p spectra of unreacted and carbonate-bearing samples at various experimental conditions using 0.1 M Na₂EDTA chelating agent + 2 M NaHCO₃

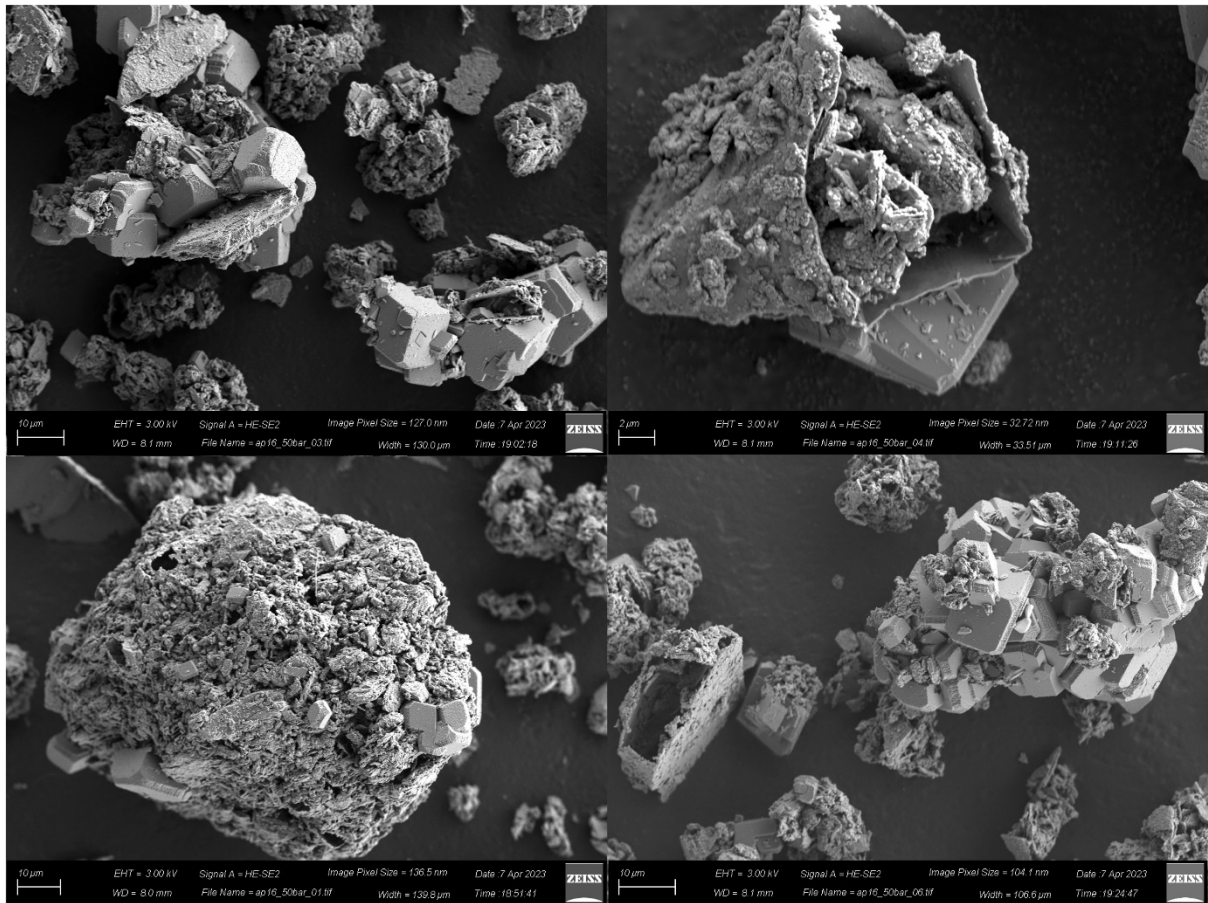


Figure S3. Characterization of morphological changes in carbonate-bearing solids using SEM showing weathered and broken crystals of magnesite reacted for 10 hours at $P_{CO_2} = 50$ bars and $185^\circ C$ using $0.1 M Na_2EDTA$ chelating agent + $2 M NaHCO_3$, slurry density of 15 wt% and a stirring speed of 500 rpm. These reactions conditions correspond to Case III.

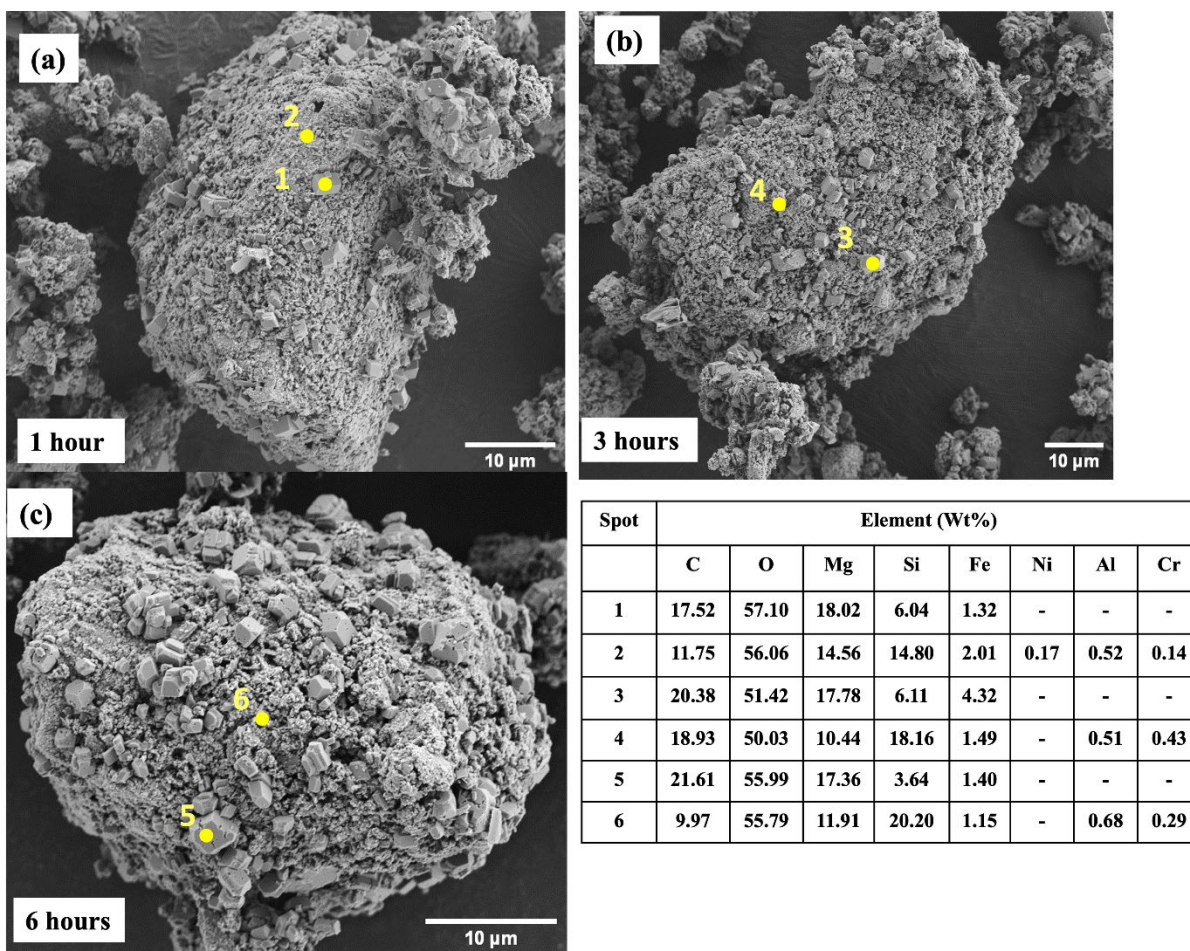


Figure S4. SEM-EDS characterization of the morphological changes in carbonate-bearing solids using SEM showing the amorphous silica-rich coating over solids reacted for (a) 1 hour (b) 3 hours and (c) 6 hours at $P_{CO_2} = 50$ bars and $185\text{ }^\circ\text{C}$ using $0.1\text{ M Na}_2\text{EDTA}$ chelating agent + 2 M NaHCO_3 , slurry density of $15\text{ wt}\%$ and a stirring speed of 500 rpm .

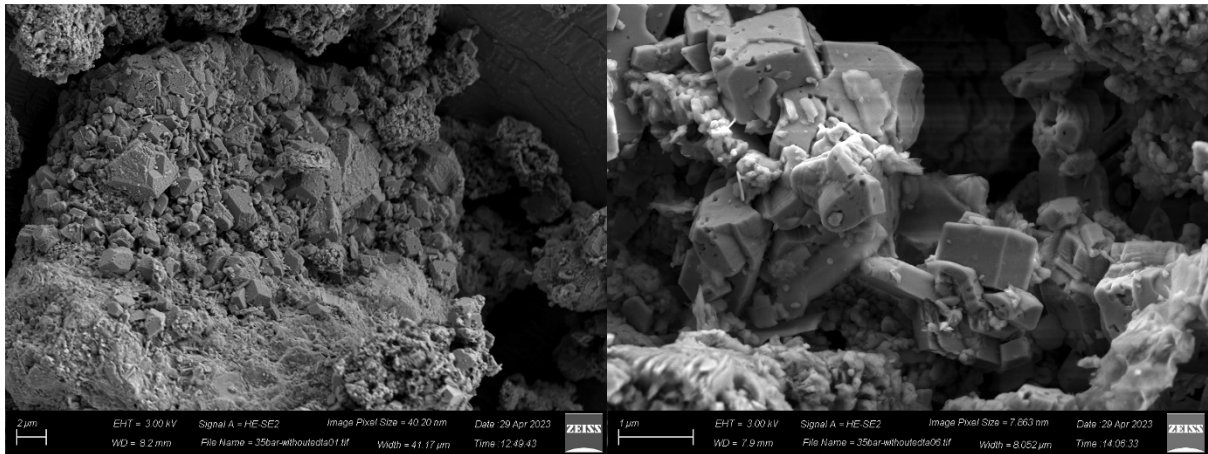
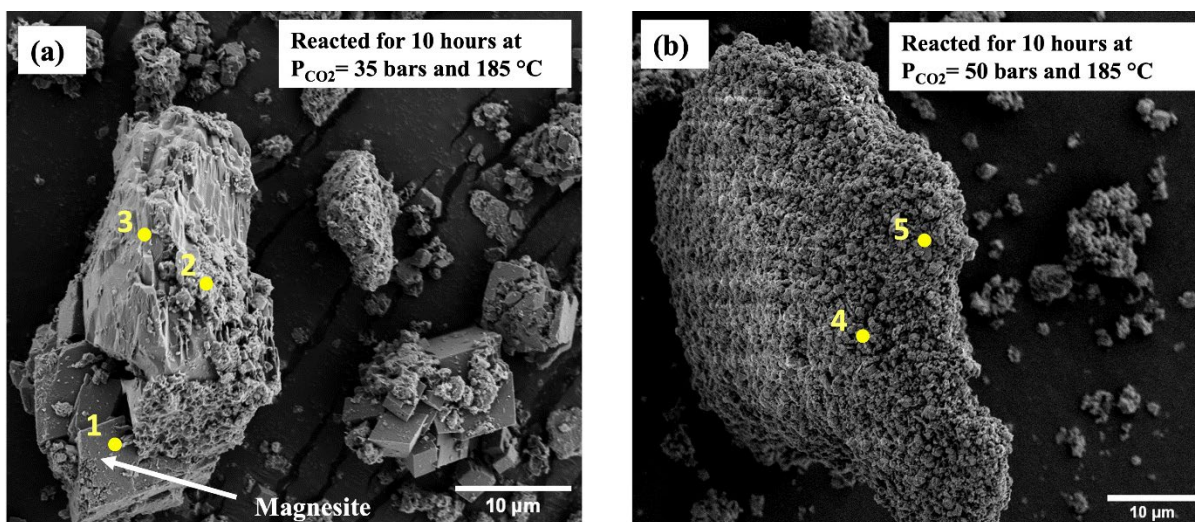


Figure S5. Characterization of morphological changes in carbonate-bearing solids using SEM showing the weathered quality of magnesite crystals after reacting for 18 hours at $P_{CO_2} = 35$ bars and $185\text{ }^{\circ}\text{C}$ using $0.1\text{ M Na}_2\text{EDTA}$ chelating agent + 2 M NaHCO_3 , slurry density of 15 wt% and a stirring speed of 500 rpm.



Spot	Element (Wt%)						
	C	O	Mg	Si	Fe	Ni	Al
1	19.25	57.25	19.73	0.19	3.58	-	-
2	22.23	48.98	15.38	9.75	3.41	0.25	-
3	13.31	44.31	22.77	13.62	6.00	-	-
4	24.01	57.32	11.13	5.71	1.66	-	0.17
5	27.32	49.64	8.96	12.08	1.72	-	0.27

Figure S6. SEM-EDS characterization of morphological changes in carbonate-bearing solids using SEM in the absence of EDTA chelating agent showing the presence of magnesite and amorphous silica-rich phases when (a) reacted for 10 hours at $P_{CO_2} = 35$ bars and $185\text{ }^\circ\text{C}$ and (b) reacted for 10 hours at $P_{CO_2} = 50$ bars and $185\text{ }^\circ\text{C}$ in the presence of 2 M NaHCO_3 , slurry density of $15\text{ wt}\%$ and a stirring speed of 500 rpm .

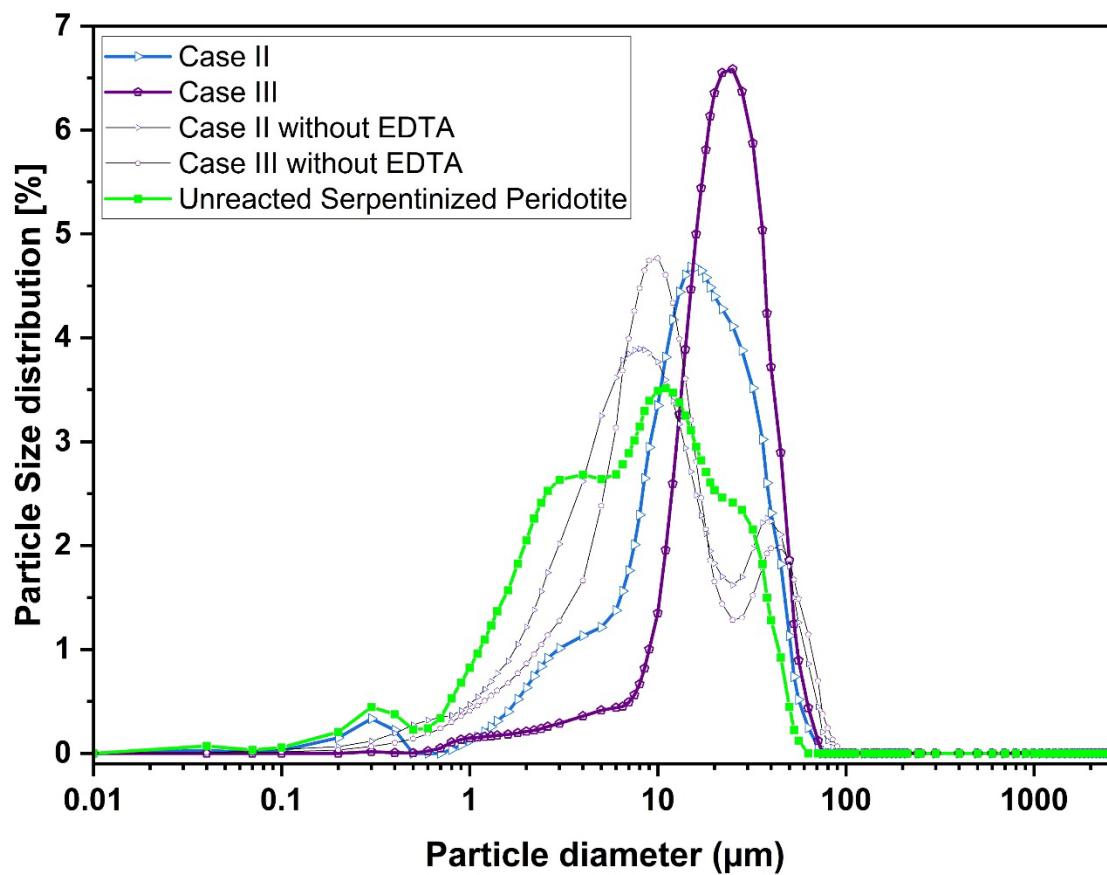


Figure S7. Comparison of particle size distributions between unreacted serpentinized peridotite and the carbonate-bearing solids for Case II and Case III, both with and without the presence of the organic ligand EDTA.

Table S1. Description of various reaction parameters for experiments conducted in this study.

Reactions	CO ₂ Partial Pressure (bars)	Reaction Temperature (°C)	Reaction Time (Hours)	Chemical Additives
1	35	155	5	2 M NaHCO ₃ ; 0.1 M Na ₂ EDTA
2		185	10	
3			18	
4	50	185	1	
5			3	
6			6	
7			10	
8	35	185	10	2 M NaHCO ₃
9	50	185	10	2 M NaHCO ₃

Table S2. Phase quantification of unreacted and reacted samples using XRD analysis

	Forsterite	Serpentine (Antigorite)	Magnesite	Other minor phases	Serpentine : Forsterite	Serpentine : Magnesite
Raw Serpentinized peridotite	56.50 ± 1.76	36.85 ± 3.85	0	6.65 ± 2.98	0.65	0.00
Case I	23.10 ± 2.81	26.50 ± 3.56	45.20 ± 4.83	5.20 ± 1.76	1.15	0.59
Case II	11.97 ± 3.15	23.10 ± 5.13	49.76 ± 7.44	15.17 ± 3.89	1.93	0.46
Case III	0.95 ± 0.32	16.20 ± 6.57	62.26 ± 8.30	20.58 ± 6.93	17.05	0.26

Table S3. XPS determined binding energies (eV) for unreacted and carbonate-bearing samples

Element	Si				C					O				Mg			O/Si	Mg/Si		
Case	2p	2p 1/2	2p 3/2	Atomic wt %	1s				Atomic wt %	1s				Atomic wt %	1s			Atomic wt %	atomic %	atomic %
Unreacted Sample	102.7	102.9	102.1	14.38	284.8	284.8	286.5	289	7.66	531.8	530.6	531.5	532.6	55.24	1303.76	1303.8	1304.28	22.4	3.84	1.56
Case I	103	103.8	102.9	20.95	285	284.8	287	289.6	5.9	532	531.5	532.4	533.3	55.42	1304	1304.7	1305.64	17.66	2.65	0.84
Case II	103.54	103.9	103.2	24.02	285.5	284.8	286.4	289.9	7.57	532.5	531.2	532.6	533.7	57.18	1304.54	1304.38	1304.75	10.89	2.38	0.45
Case III	103.63	104	103.1	25.82	289.6	284.8	286.6	289.7	8.72	532.6	531.4	532.5	533.5	59.34	1304.63	1304.12	1304.84	5.87	2.30	0.23

Table S4. Stability constant ($\log K_{ML}$) of metal-EDTA complex ions in aqueous solution (Wang and Dreisinger, 2022; Martell and Smith, 1974).

Cations	Mg ²⁺	Ca ²⁺	Fe ²⁺	Co ²⁺	Ni ²⁺	Fe ³⁺	Cr ²⁺	Cr ³⁺
$\log K_{ML}$ of metal-EDTA complex ions	8.69	10.69	14.32	16.31	18.62	25.1	13.6	23.4

Table S5. Thermodynamic properties of common minerals in ultramafic formations at different reaction conditions (Robie and Hemingway, 1995)

Common Minerals in Ultramafic Formations	Chemical Formula	298.15 k and 1 Bar						458.15 k and 1 Bar		
		Weight	Entropy	Volume	Enthalpy	Free Energy	Log(K _f)	Enthalpy	Free Energy	Log(K _f)
			S°	V°	Δ _f H°	Δ _f G°		Δ _f H°	Δ _f G°	
		gm	J.mol ⁻¹ .K ⁻¹	cm ³	kJ.mol ⁻¹	kJ.mol ⁻¹		kJ.mol ⁻¹	kJ.mol ⁻¹	
Bunsenite	NiO	74.69	-	-	-239.3	-211.1	37.0	-236.8	-190.9	19.2
heazlewoodite	Ni ₃ S ₂	240.20	-	-	-344.9	-289.9	50.8	-343	-253.1	26.4
Siderite	FeCO ₃	115.86	95.5	29.38	-755.9	-682.8	119.6	-754	-633.8	66.2
Hematite	Fe ₂ O ₃	159.69	87.4	30.27	-826.2	-744.4	130.4	-822.3	-689.9	72.1
Trevorite	NiFe ₂ O ₄	232.38	140.9	43.65	-1070.5	-965.1	169.1	-1066.4	-894.8	93.5
Magnetite	Fe ₃ O ₄	231.53	146.1	44.52	-1115.7	-1012.7	177.4	-1109.2	-944.5	98.7
Magnesite	MgCO ₃	84.31	65.1	28.02	-1113.3	-1029.5	180.4	-1111.9	-973	101.7
Calcite	CaCO ₃	110.87	91.7	36.93	-1207.4	-1128.5	197.7	-1204.9	-1075.6	112.4
Spinel	Ni ₂ SiO ₄	209.46	124.1	39.81	-1389.7	-1280.9	224.4	-1389.1	-1207.3	126.1
Chromite	FeCr ₂ O ₄	223.83	146	44.01	-1445.5	-1344.5	235.5	-1443.4	-4576.6	133.4
Spinel	MgAl ₂ O ₄	142.26	88.7	39.71	-2299.1	-2176.6	381.3	-2299.8	-2093.3	218.7

References

Martell, A.E. and Smith, R.M., 1974. *Critical stability constants* (Vol. 1, p. 135). New York: Plenum press.

Robie, R.A. and Hemingway, B.S., 1995. *Thermodynamic properties of minerals and related substances at 298.15 K and 1 bar (105 Pascals) pressure and at higher temperatures* (Vol. 2131). US Government Printing Office.

Wang, F. and Dreisinger, D., 2022. Carbon mineralization with concurrent critical metal recovery from olivine. *Proceedings of the National Academy of Sciences*, 119(32), p.e2203937119.